Japanese Journal of Applied Physics

The Japan Society of Applied Physics

PROGRESS REVIEW • OPEN ACCESS

Ga vacancies in β-Ga_2O_3: split or not?

To cite this article: Filip Tuomisto 2023 *Jpn. J. Appl. Phys.* **62** SF0802

View the article online for updates and enhancements.

You may also like

- High-density magnetic-vacancy inclusion in Co_2MnGa single crystal probed by spin-polarized positron annihilation spectroscopy
A Miyashita, M Maekawa, Y Shimoyama et al.

- Spin-polarized annihilation lifetime of positron of d^0 ferromagnetism in gallium nitride: A two-component density functional theory simulation
Satoshi Hagiwara, Yasumitsu Suzuki and Kazuyuki Watanabe

- X-ray absorption study of defects in reactively sputtered GaN films displaying large variation of conductivity
Mohammad Monish, C Nayak, D S Sutar et al.

This content was downloaded from IP address 128.214.173.198 on 02/06/2023 at 15:58

OPEN ACCESS

Japanese Journal of Applied Physics **62**, SF0802 (2023)

https://doi.org/10.35848/1347-4065/acc7b1

PROGRESS REVIEW

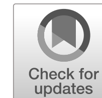

Ga vacancies in β-Ga_2O_3: split or not?

Filip Tuomisto[*]

Department of Physics and Helsinki Institute of Physics, University of Helsinki, POB 43, FI-00014 Helsinki, Finland

[*]E-mail: filip.tuomisto@helsinki.fi

Received December 30, 2022; revised March 21, 2023; accepted March 26, 2023; published online April 19, 2023

Ga vacancies and their unusual structure in β-Ga_2O_3 have been studied in recent years by several experimental techniques as well as theoretical calculations. Theory predicts that the so-called split Ga vacancy configuration is the one with the lowest formation energy. Positron annihilation spectroscopy faces challenges with β-Ga_2O_3 due to the colossal signal anisotropy and lack of a proper reference sample. Nevertheless, the majority of the data strongly suggests that all studied β-Ga_2O_3 samples contain high concentrations of split Ga vacancies in a wide distribution of configurations. EPR, IR spectroscopy and scanning transmission electron microscopy experiments all agree on the split Ga vacancy configuration as being the most likely interpretation of the data. However, the exact structure of the split Ga vacancies remains to be solved in terms of complexes with O vacancies and hydrogen. © 2023 The Author(s). Published on behalf of The Japan Society of Applied Physics by IOP Publishing Ltd

1. Introduction

Interest in β-Ga_2O_3 has seen a strong increase in the past decade thanks to its ultra-wide energy gap (4.6–4.9 eV) and high critical field (6–8 MV cm^{-1}).[1] In addition, it is possible to grow large-area high quality bulk single crystals.[2] Unipolar devices have been developed, and controlled n-type doping is the key to achieving the desired properties.[3–5] Detailed identification of dominating lattice defects is an important goal in order to further improve the properties of β-Ga_2O_3 devices.[6] Generally, the formation of acceptor-type native point defects is enhanced in n-type doped semiconductors but in most compound semiconductors this does not limit the carrier concentration.[7–10] In this review, the focus is on Ga vacancy related defects as they have acceptor character and hence ought to be efficient compensating centers, while O vacancy related defects have deep donor character.[6]

Theoretical calculations of defect properties in β-Ga_2O_3 predict unusually low—even negative—formation energies for Ga vacancy related defects in all of their negative charge state configurations at Fermi levels near the conduction band edge.[11–14] This suggests that Ga vacancy defects should be abundant and efficiently compensate for the n-type doping. Even complexes involving a Ga vacancy, O vacancy, and two hydrogen atoms are predicted to exhibit negative charge states at high Fermi levels. There is also abundant experimental evidence obtained by IR spectroscopy, EPR spectroscopy, positron annihilation spectroscopy and transmission electron microscopy that (split) Ga vacancies are present at very high concentrations in β-Ga_2O_3.[15–18] Theory also predicts that these split Ga vacancies have the lowest formation energies.[11–14] Three different split Ga vacancy configurations have been shown to form, where a next-nearest neighbor fourfold coordinated Ga(1) atom relaxes inwards into the interstitial space, as depicted in Fig. 1. The resulting split Ga vacancy has an open volume on both sides of the center interstitial, resulting in two "half-vacancies." The split Ga vacancy $V_{Ga}{}^{ia}$ forms at Ga(1) and Ga(2) sites, while $V_{Ga}{}^{ib}$ and $V_{Ga}{}^{ic}$ are formed by two Ga(1) sites. It should be noted that the split Ga vacancies are monovacancies as they involve only one missing atom. Why these defects are not efficient in compensation of the donors, allowing for controllable n-type doping, remains an open question.

This progress review focuses on the question of the dominant form of existence of Ga vacancy related defects in β-Ga_2O_3: split or not? In addition, the possible formation of complexes with oxygen vacancies, hydrogen, and n-type dopants is discussed in the light of theoretical predictions and experimental evidence. Experimental results obtained with positron annihilation spectroscopy are given particular attention.

2. Positron annihilation spectroscopy

Positron annihilation spectroscopy has particular use in the identification and quantification of vacancy-type defects in semiconductors in the concentration range 10^{15}–10^{19} cm^{-3}.[19] It is possible to distinguish between different charge states of the vacancies and give information on their chemical environment, in addition to the size of the open volume and the concentrations. In the experiments, positrons are implanted into the sample material where they eventually annihilate with electrons emitting two 511 keV γ-photons. The positrons probe the interstitial space in a delocalized state in the crystal lattice and may get trapped at open volume defects thanks to the missing repulsive ion core. The trapping at vacancies causes changes in the positron-electron annihilation radiation: the positron lifetime and the Doppler broadening of the 511 keV annihilation line. The positron lifetime increases when the positron is trapped in a vacancy. Usually positron trapping at vacancies is detected as a narrowing of the Doppler broadened 511 keV line. Generally, the positron lifetime gives information about the open volume and concentration of the vacancy defects, while Doppler broadening gives information on the chemical surroundings of the vacancy, namely the electron configuration of the surrounding atoms. Interestingly, in β-Ga_2O_3 the Doppler broadening signal anisotropy is colossal compared to other semiconductors, allowing for novel types of experiments.[17]

2.1. Experiment

The standard approach for studying bulk crystals is sandwiching a low-activity ^{22}Na positron source between two

Content from this work may be used under the terms of the Creative Commons Attribution 4.0 license. Any further distribution of this work must maintain attribution to the author(s) and the title of the work, journal citation and DOI.

© 2023 The Author(s). Published on behalf of The Japan Society of Applied Physics by IOP Publishing Ltd

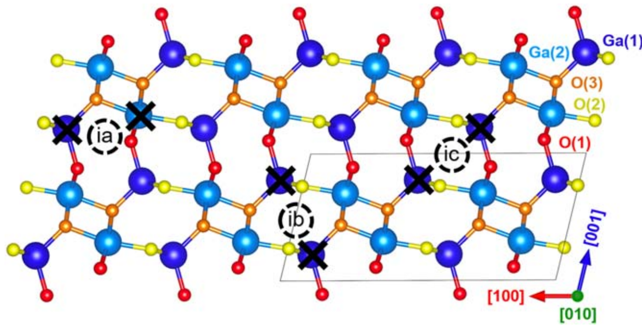

Fig. 1. Structures of the split Ga vacancies in the β-Ga_2O_3 lattice. The [010] direction is out of the plane and towards the reader. The different Ga and O sites are marked with different colors. The cation monovacancies in β-Ga_2O_3 have the special property that the regular monovacancies, V_{Ga1} and V_{Ga2}, easily relax into three different configurations $V_{Ga}{}^{ia}$, $V_{Ga}{}^{ib}$ and $V_{Ga}{}^{ic}$. In these defects a neighboring fourfold coordinated Ga(1) atom relaxes inwards into the interstitial space. The resulting split Ga vacancy has an open volume on both sides of the center interstitial, resulting in two "half-vacancies." The split Ga vacancy $V_{Ga}{}^{ia}$ forms at Ga(1) and Ga(2) sites, while $V_{Ga}{}^{ib}$ and $V_{Ga}{}^{ic}$ are formed by two Ga(1) sites. The split Ga vacancies are monovacancies as they involve only one missing atom.

identical pieces of the sample material. The fast positrons emitted by the source probe the sample up to about 200 μm providing averaged data over these depths. Thin films can be studied with a slow positron beam where the positrons emitted by the source are slowed down and implanted in a single sample at kinetic energies up to 40 keV, probing the near-surface region up to 2 μm below the surface. For a detailed account on the experimental techniques, see Ref. 19).

The positron lifetime experiment represents the probability distribution of positron annihilation at time t and is analyzed as a superposition of exponential decay components: $n(t) = \sum_i I_i e^{-t/\tau_i}$ convoluted with the Gaussian resolution function of the spectrometer. A positron in state i annihilates with a specific lifetime τ_i, while the intensity I_i depends on the fraction of positrons annihilating in state i. The average lifetime $\tau_{ave} = \sum_i I_i \tau_i$ is typically used as an experimental parameter as it coincides with the center of mass of the lifetime spectrum and has very high statistical accuracy thanks to the $>10^6$ collected annihilation events. Typically, the lifetime is 20%–50% longer for a positron trapped at a vacancy than for a positron in the delocalized state in the lattice (e.g. 160 ps for the lattice and 235 ps for the Ga vacancy in GaN[7]).

The motion of the annihilating electron-positron pair causes a Doppler shift in each annihilation event $\Delta E = cp_L/2$, where p_L is the longitudinal momentum component of the pair in the direction of the annihilation photon emission. The shape of the 511 keV peak gives thus the one-dimensional momentum distribution of the annihilating electron-positron pairs as shown schematically in Fig. 2. A Doppler shift of 1 keV corresponds to a momentum value of $p_L = 0.54$ a.u. Due to limited resolution and a relatively low peak-to-background ratio ($\sim 10^2$ on the right hand side of the peak) in conventional experiments, integrated parameters are used to describe the shape of the Doppler-broadened annihilation peak. The low electron-momentum parameter S is defined as the ratio of the counts in the central region (typically $p_L < 0.4$ a.u.) of the annihilation line to the total number of counts in the line. The high electron-momentum parameter W is the fraction of the counts in the wing regions of the line (typically $p_L > 1.5$–2.0 a.u.). Typically, the S parameter increases by 3%–5% when positrons annihilate as trapped at vacancies, while the decrease of the W parameter is 15%–50%.

As discussed in detail in Refs. 17 and 20, it is important to note that the data obtained in Doppler broadening experiments are by definition dependent on the measurement direction relative to the crystal orientation. Typically the "longitudinal" measurement direction mentioned above is along a crystal orientation within the sample surface or perpendicular to it (see Fig. 2). When performing defect studies in "conventional" semiconductors with Doppler broadening, the measurement orientation is usually disregarded as the relative differences in the signals in the different directions are at most of the order of 0.05%–0.1% and hence negligible. However, β-Ga_2O_3 is colossally different in this respect. Relative changes of the S parameter as high as 4% have been measured by rotating the samples. The root cause lies in the quasi-one-dimensional positron state in the β-Ga_2O_3 lattice,[17] but the detailed mechanisms giving rise to the unusually high anisotropy are still to be elucidated. While this phenomenon causes severe challenges to the interpretation of the results as the magnitude is similar to typical vacancy-induced changes, it also allows for novel approaches for defect identification with positron annihilation.

For defect identification, the measured (S, W) parameters are typically plotted in a plane as illustrated in Fig. 3. This figure highlights the anisotropy issue faced when studying β-Ga_2O_3. In "conventional" semiconductors such as GaAs or GaN, the annihilations in the defect-free lattice (bulk) and at cation vacancies produce clearly different signals and the data are straightforward to interpret.[19] Changing the measurement orientation for these materials produces changes in the parameters that are smaller than the symbol size in the figure. However, in β-Ga_2O_3, the full extent of the measured anisotropy is larger than the largest predicted distance between bulk and a mono-vacancy (unrelaxed V_{Ga1}) along a single orientation, in this case [100].[17]

2.2. Theory

An important advantage of positron annihilation spectroscopies is the possibility of predicting the annihilation signals from first principles.[19] Delocalized and trapped positron states and their associated lifetimes are modeled using two-component density functional theory for electron-positron systems. The local density approximation employed for the correlation potential and enhancement factor typically predicts too high annihilation rates with 3d electrons in comparison with the experiments, but differences and ratios in positron lifetimes and Doppler spectra can be compared with high confidence.[21,22] For comparison with experiments, the three-dimensional momentum density is first projected into the desired crystal direction and then convoluted with the experimental detector resolution function. A detailed description of the annihilation parameter modeling applied to β-Ga_2O_3 is found in Ref. 17).

3. Results and discussion

3.1. Positron experiments in β-Ga_2O_3

Reports of positron experiments in β-Ga_2O_3 can be divided into two categories. The first category (also chronologically)

© 2023 The Author(s). Published on behalf of
The Japan Society of Applied Physics by IOP Publishing Ltd

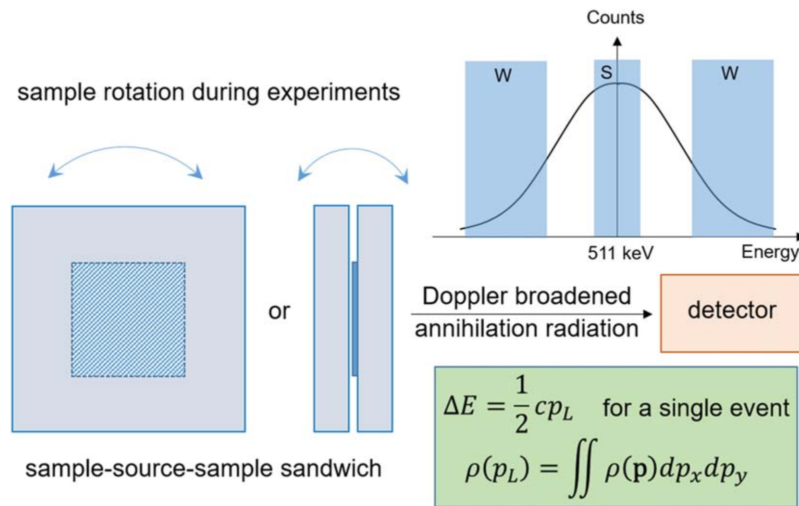

Fig. 2. The Doppler broadening measurement with fast positrons in the so-called 3D configuration, where the sample-source-sample sandwich is rotated with respect to the measurement direction. Each annihilation event contains the information (Doppler shift) of the momentum of the annihilation electron-positron pair projected along the direction of measurement. Detecting a large number of events (order of magnitude 10^6) leads to a Doppler-broadened 511 keV energy line that represents the momentum distribution of the annihilating electrons that carry most of the momentum. The *S* and *W* parameters describe the shape of this line.

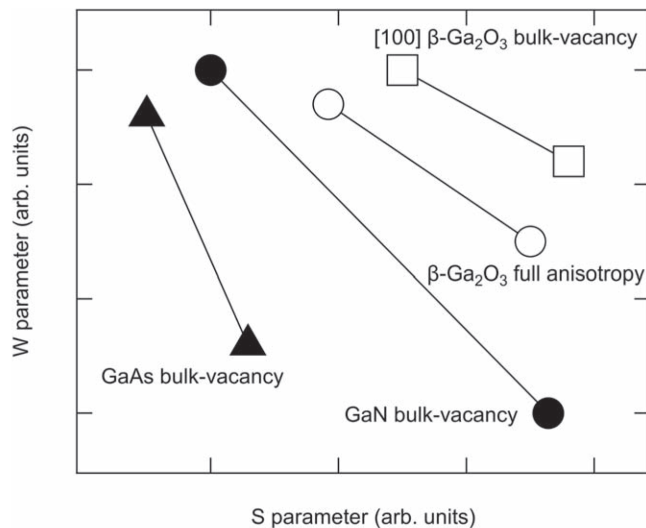

Fig. 3. Illustration of differences in (*S*, *W*) parameters of the defect-free lattice (bulk) and Ga vacancy in GaAs, GaN, and β-Ga_2O_3.[17,19] The data for different materials are shown in arbitrary units and shifted with respect to one another to show the relative differences. The anisotropy or measurement orientation dependence of the (*S*, *W*) parameters in GaAs and GaN is smaller than the symbol size. In β-Ga_2O_3, the largest predicted bulk-vacancy difference that is predicted to occur for the V_{Ga1} in measurement along [100] is smaller than the full measured anisotropy.

consists of experiments where the anisotropy of the Doppler broadening signals is not considered, either due to performing only lifetime experiments or due to the lack of knowledge of the unusual properties of β-Ga_2O_3. The second category consists of experiments where the colossal anisotropy of the Doppler broadening signals is acknowledged, leading also to the realization that the split Ga vacancy configuration is the key to interpreting most of the experimental results.

The early work on β-Ga_2O_3 with positron annihilation spectroscopy consists of positron lifetime experiments in sintered polycrystalline material, with a single crystal as a reference point.[23,24] Large open volume defects were found in the polycrystalline samples, but the single crystal produced a single positron lifetime of roughly 180 ps that was interpreted as the "bulk" lifetime, or the lifetime of delocalized positrons in the β-Ga_2O_3 lattice. A similar single lifetime (176 ps) was found also in the single crystal substrate in the work performed after the interest in β-Ga_2O_3 was revived, still interpreted as the bulk lifetime.[25] Large vacancy clusters have also been observed by positron lifetime experiments recently, both in sintered bulk samples and in annealed hetero-epitaxial thin films.[26–28]

Doppler broadening experiments were the main approach used to study the possible involvement of Ga vacancies in the electrical compensation of n-type doping in hetero- and homo-epitaxial β-Ga_2O_3 thin films in Ref. 25). With the lack of earlier positron annihilation studies on defects in β-Ga_2O_3, the interpretations were based on comparison to well-known phenomena in GaN and ZnO. The anisotropy of the Doppler broadening signals was not considered, and also the possible strong relaxation of the Ga vacancies was ignored. The data strongly suggested that the (unrelaxed) Ga vacancy defects would be present at high concentrations in semi-insulating Si-doped and undoped thin films, providing an explanation for the electrical compensation. This interpretation was later reinforced by experiments in Sn-doped n-type thin films where the Ga vacancy concentrations were found to be very low.[29] However, the controversy in relation to theoretical predictions remained: Ga vacancy concentrations were found to be low in n-type material and high in semi-insulating material, while theory pointed towards the opposite.

The work on the effect of alloy composition and Si doping on vacancy defects in $(In_xGa_{1-x})_2O_3$ thin films was also performed without knowledge of the unusual anisotropy effects exhibited by the Doppler broadening signals in β-Ga_2O_3.[30] Detailed investigations of these effects could shed more light on the delicate balance between the different phases in the continuous-composition spread samples used in the studies.

The colossal anisotropy of the Doppler broadening signals in β-Ga_2O_3 was revealed only very recently.[17] This finding

© 2023 The Author(s). Published on behalf of The Japan Society of Applied Physics by IOP Publishing Ltd

was accompanied by the observation that all bulk crystals and homo-epitaxial thin films exhibit this anisotropy.[31] In addition, the experimental anisotropy was found to be significantly larger than that predicted by theoretical calculations for the β-Ga_2O_3 lattice. Instead, the anisotropy predicted for various split Ga vacancy configurations[11–14] was found to be comparable to the experiments. This is another highly unusual property of β-Ga_2O_3: in other semiconductors the vacancy related Doppler broadening signals are more isotropic than those of the lattice.

The colossal anisotropy of the positron Doppler broadening signals measured in all β-Ga_2O_3 crystals does not depend on the doping. It is found in undoped, Mg-doped, Fe-doped, Sn-doped, indicating that all these crystals contain high concentrations of split Ga vacancies.[31] However, the configuration distributions are different in the different crystals, as revealed by temperature-dependent positron lifetime experiments.[31] It is remarkable that the measured lifetimes in the as-grown crystals are in the range 175–185 ps, coinciding with the earlier interpretation as "bulk." It is, however, now evident that this lifetime corresponds to the split Ga vacancies. Theoretical calculations predict 10–30 ps longer lifetimes for the split Ga vacancies (in various configurations, including O vacancies and H decoration) than in the lattice, suggesting that the true lattice positron lifetime in β-Ga_2O_3 is clearly shorter than 170 ps.[17,31,32] Hydrogen implantation experiments and subsequent annealings reveal a complex interplay between hydrogen, split Ga vacancies, and potentially also unrelaxed Ga vacancies.[32] In particular, the latter observation requires further studies for a more detailed picture as theory predicts the unrelaxed Ga vacancy to be a metastable configuration with a relatively low (less than 1 eV) barrier for relaxation.[11]

Figure 4 shows the average positron lifetime measured in a Fe-doped β-Ga_2O_3 crystal grown by the edge-defined film-fed method.[31] This crystal produces the shortest positron lifetimes measured so far. The grey shadow behind the markers shows the variation in the early experimental assignments of the bulk lifetime. The temperature dependence of the average positron lifetime in the Fe-doped crystal is a clear indication of the data being dominated by (negatively charged) vacancies,[19] even if the exponential decay profile contains only a single component. This alone demonstrates that the vacancy concentrations are high even in this sample, although the lifetime is shorter than the early assignments of the bulk lifetime. The blue shadow shows the range of values of the average positron lifetime measured in polycrystalline material, corresponding to relatively large vacancy clusters.[24,26–28] Preliminary experiments after subjecting the Fe-doped crystal to ion irradiation give a range of average lifetime values given by the red shadow in Fig. 4. Theoretical calculations suggest that the positron lifetime should be 15–20 ps longer in unrelaxed than in split Ga vacancies. Hence, if the average positron lifetime in the Fe-doped crystal corresponds to the split Ga vacancies it is possible that irradiated samples contain unrelaxed Ga vacancies.

The colossal anisotropy of the Doppler broadening signals makes it extremely important to pay close attention to the measurement direction and give a detailed account of the measurement geometry in any Doppler broadening experiment performed in β-Ga_2O_3. Together with the lack of a

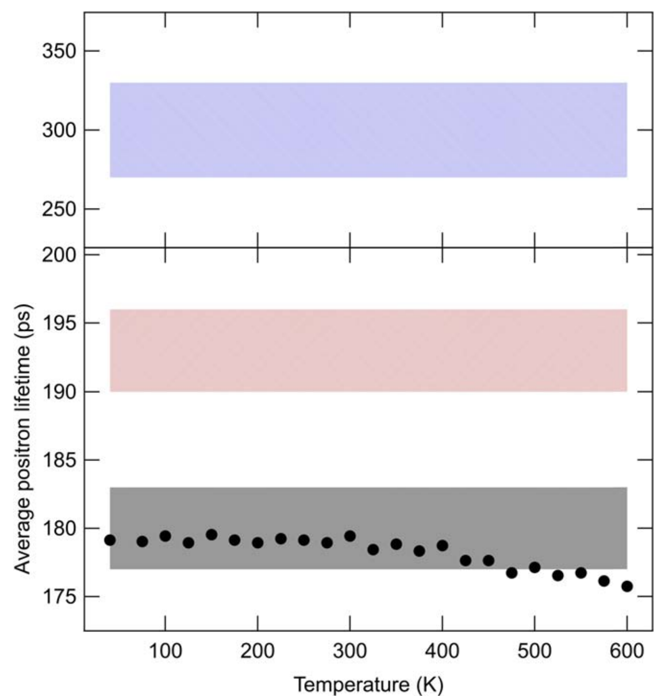

Fig. 4. The lower panel shows the average positron lifetime measured in Fe-doped β-Ga_2O_3 (black markers).[32] The grey shaded areas show the variation in the early experimental assignments of the bulk positron lifetime in β-Ga_2O_3.[23–25] The red shaded area shows the range of the values of the average positron lifetime obtained in preliminary experiments in ion irradiated Fe-doped β-Ga_2O_3. The blue shaded area in the top panel shows the range of average positron lifetime values measured in polycrystalline samples.[23–28] The data are shown as shadows for illustrative purposes as most of the experimental data has been obtained only at RT.

proper "defect-free" reference sample, making useful interpretations concerning defect identities or concentrations requires the use of unusual approaches. Analyzing the anisotropy itself provides access to the detailed identities.[17,31,32] Another approach is to make a detailed analysis of the positron diffusion lengths in slow positron experiments.[33–35] This gives the possibility to interpret the changes in terms of defect concentrations, but also there the anisotropy needs to be acknowledged. It is not yet known whether the quasi-one-dimensional positron state in the β-Ga_2O_3 lattice causes anisotropy in positron diffusion as well.

3.2. Discussion

Positron annihilation spectroscopy is generally considered a powerful method for detailed identification and quantification of vacancy-type defects in semiconductors. However, this is based on two conditions: (1) the existence of a suitable reference sample that can be considered defect-free from the perspective of positrons, hence producing annihilation signals of the lattice (usually called "bulk"), and (2) the dominance of a single type of defect in the annihilation signals, at least in some externally controllable state of the sample(s). When these conditions are fulfilled, it is reasonably straightforward to interpret both the positron lifetime and Doppler broadening signals through comparison with state-of-the-art theoretical calculations.[19] In particular, the Doppler broadening data are typically presented as normalized by the data in the reference sample, both when presenting (S, W) plots or coincidence Doppler data as ratio curves for identifying the fingerprints of the various defects.

© 2023 The Author(s). Published on behalf of The Japan Society of Applied Physics by IOP Publishing Ltd

Figure 3 illustrates the concept of an (*S*, *W*) plot. For example, if GaN samples with varying concentrations of Ga vacancies are analyzed, the data points will fall on the line connecting the "bulk" and vacancy points (black circle markers) and the positioning on the line is directly dependent on the defect concentration.

As is evident from the results reported so far in β-Ga_2O_3, neither of the two conditions is fulfilled. Theoretical predictions for the typical fingerprints have been published,[17,31,32] with the hope that future research efforts leading to having suitable samples. In the meantime, the colossal anisotropy of the Doppler broadening signals can be utilized for making rather strong—although somewhat qualitative—arguments concerning the structure of the Ga vacancy defects as well as their concentrations. Importantly, the general form and span of the anisotropy indicate that trapping at split Ga vacancies is responsible for a significant fraction of positron annihilation signals in all studied β-Ga_2O_3 samples.[31] This means that their concentrations are well above 10^{18} cm^{-3}. However, the relative differences between the differently doped materials and the nontrivial behavior of the positron lifetime as a function of temperature [see Ref. 31)] indicate that all of the samples contain more than just one type of split Ga vacancy defect at significant concentrations. Based on the positron data, it is highly likely that the in-grown split Ga vacancies are present in the form of different types of complexes with O vacancies and hydrogen, in addition to the different configurations of the "clean" split Ga vacancy.[11–14]

Figure 5 shows the (*S*, *W*) parameters in selected samples measured along different crystal orientations: Fe-doped and Sn-doped single crystals grown by EFG (edge-defined film-fed growth) and a Mg-doped single crystal grown by the Czochralski method.[31] The surface orientation of the EFG samples is (001) and the Czochralski crystal is (100). The data have been adjusted for the different detector resolutions and measurement geometries (by measuring some of the crystals with several setups) so that they can be shown in the same figure. To highlight the evolution of the anisotropy in the (*S*, *W*) data, points measured between the high-symmetry crystal orientations in the Mg-doped Czochralski crystal are also shown.[17] As pointed out above, the data cannot be normalized to a well-defined reference point. Hence Fig. 5 shows the "raw" *S* and *W* parameters. The purple, black and green bars in the figure represent the calculated overall anisotropy of a typical split Ga vacancy, the β-Ga_2O_3 lattice, and an unrelaxed Ga vacancy, respectively.[17] It is clear from the figure that the experimental anisotropy is significantly larger than that calculated for the β-Ga_2O_3 lattice (or the unrelaxed Ga vacancies), irrespective of the sample. This is a strong indication of the experimental signals being dominated by positrons annihilating as trapped at split Ga vacancies. Interestingly, preliminary results in the ion irradiated Fe-doped EFG crystal suggest that the overall anisotropy is strongly reduced. In combination with the positron lifetime obtained in the crystal (see Fig. 3) it is likely that this crystal contains unrelaxed Ga vacancies.

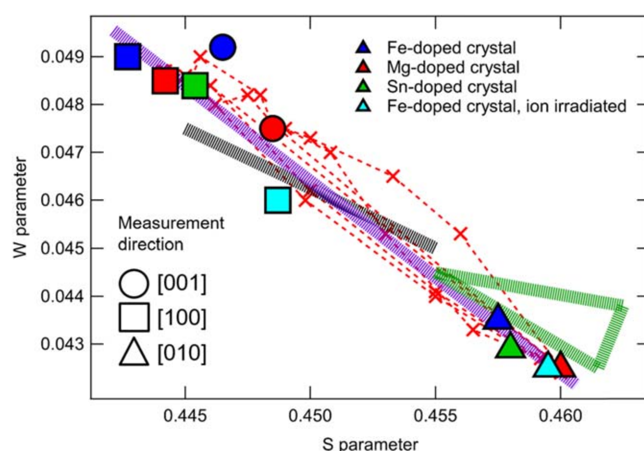

Fig. 5. Experimentally determined (*S*, *W*) parameters for various β-Ga_2O_3 samples.[31] The data have been adjusted for the differences in the energy resolutions and measurement geometries in different setups. The marker size corresponds to the experimental error bar. The purple, black, and green shadowed scale bars represent the overall anisotropy obtained with theoretical calculations of a typical split Ga vacancy, the β-Ga_2O_3 lattice, and an unrelaxed Ga vacancy, respectively. The circle, square and triangle markers correspond to the [001], [100] and [010] measurement directions. The red crosses connected by a dashed line show the values measured along great circles between these three directions in the Mg doped crystal.

The fact that EPR experiments have only been reported for irradiation or high temperature annealing induced defects in β-Ga_2O_3 supports the interpretation that the in-grown Ga vacancies are present as complexes rather than isolated.[16,36–39] The EPR experiments appear to agree that these defects are in the doubly negative charge state, hence acting as compensating centers for n-type conductivity. There is an ongoing debate on whether the EPR signals originate from unrelaxed or split Ga vacancies, but comparing experiments with state-of-the-art theoretical calculations suggests that the irradiation-induced Ga vacancies are in the split configuration.[37] IR absorption spectroscopy is extremely powerful in identifying hydrogen-related defect centers, and has been applied to β-Ga_2O_3 in recent years.[15,40–43] The experiments are typically performed on samples with hydrogen and/or deuterium introduced by diffusion or ion implantation. The observed vibrational modes are consistent with split Ga vacancy configurations complexed with 1–3 hydrogen or deuterium atoms, demonstrating the strong propensity of these defects to form complexes. Also split Ga vacancy—O vacancy complexes have been observed.[41] The IR experiments fully support the interpretation that in-grown Ga vacancy defects are predominantly present in the split configuration. We note that the split Ga vacancies have also been observed by scanning transmission electron microscopy (STEM), also supporting their presence at high concentrations.[18]

Combining the findings of positron annihilation spectroscopy, STEM, EPR, and IR absorption strongly suggests that in-grown Ga vacancies in β-Ga_2O_3 are present in the split Ga vacancy configuration at high concentrations, well above 10^{18} cm^{-3}. The experimental evidence also suggests that these split Ga vacancies are present as a distribution of various configurations, most likely complexed with O vacancies and hydrogen. This observation also offers a possible solution to the question of compensation, that is, why the n-type doping of β-Ga_2O_3 works so well even if the Ga vacancy concentrations are extremely high. Many of the split Ga vacancy—O vacancy—(multi-)hydrogen configurations are predicted to be neutral for a large part of the band-gap,[14] and these will not cause compensation. However, the exact structure of the dominant native defects remains to be solved and is the

© 2023 The Author(s). Published on behalf of The Japan Society of Applied Physics by IOP Publishing Ltd

subject of future work. It should be noted that it is still uncertain whether irradiation-induced Ga vacancies could also be in the unrelaxed configuration, as suggested by EPR and positron experiments.[32,36]

4. Summary

Point defects in β-Ga_2O_3 have been studied in recent years by several experimental techniques. Positron annihilation spectroscopy, a powerful method for identifying and quantifying vacancy-type defects, faces challenges with β-Ga_2O_3 due to the colossal signal anisotropy and lack of a proper reference sample. Nevertheless, the data can be interpreted as the signals being dominated by split Ga vacancy defects in all studied β-Ga_2O_3 samples. Theory predicts that the split Ga vacancy configurations have the lowest formation energies, and EPR, IR and STEM experiments all agree on the split Ga vacancy configuration as being the most likely interpretation. The exact structure of the split Ga vacancies remains to be solved in terms of complexes with O vacancies and hydrogen.

Acknowledgments

This work was partially funded by the Academy of Finland Grant No. 315082.

1) M. Higashiwaki, K. Sasaki, A. Kuramata, T. Masui, and S. Yamakoshi, Appl. Phys. Lett. **100**, 013504 (2012).
2) S. J. Pearton, J. Yang, P. H. Cary IV, F. Ren, J. Kim, M. J. Tadjer, and M. A. Mastro, Appl. Phys. Rev. **5**, 011301 (2018).
3) M. Higashiwaki, H. Murakami, Y. Kumagai, and A. Kuramata, Jpn. J. Appl. Phys. **55**, 1202A1 (2016).
4) J. Zhang, J. Shi, D.-C. Qi, L. Chen, and K. H. L. Zhang, APL Mater. **8**, 020906 (2020).
5) M. H. Wong and M. Higashiwaki, IEEE Trans. Electron Devices **67**, 3925 (2020).
6) M. D. McCluskey, J. Appl. Phys. **127**, 101101 (2020).
7) K. Saarinen et al., Phys. Rev. Lett. **79**, 3030 (1997).
8) F. Tuomisto, V. Ranki, K. Saarinen, and D. C. Look, Phys. Rev. Lett. **91**, 205502 (2003).
9) J.-M. Mäki, I. Makkonen, F. Tuomisto, A. Karjalainen, S. Suihkonen, J. Räisänen, T. Y. Chemekova, and Y. N. Makarov, Phys. Rev. B **84**, 081204(R) (2011).
10) E. Korhonen, F. Tuomisto, O. Bierwagen, J. S. Speck, and Z. Galazka, Phys. Rev. B **90**, 245307 (2014).
11) J. B. Varley, H. Peelaers, A. Janotti, and C. G. Van de Walle, J. Phys.: Condens. Matter **23**, 334212 (2011).
12) A. Kyrtsos, M. Matsubara, and E. Bellotti, Phys. Rev. B **95**, 245202 (2017).
13) C. Zimmermann, V. Ronning, Y. K. Frodason, B. Bobal, and L. Vines, Phys. Rev. Mater. **4**, 075605 (2020).
14) Y. K. Frodason, C. Zimmermann, E. F. Verhoeven, P. M. Weiser, L. Vines, and J. B. Varley, Phys. Rev. Mater. **5**, 025402 (2021).
15) P. Weiser, M. Stavola, W. B. Fowler, Y. Qin, and S. Pearton, Appl. Phys. Lett. **112**, 232104 (2018).
16) N. T. Son, Q. D. Ho, K. Goto, H. Abe, T. Ohshima, B. Monemar, Y. Kumagai, T. Frauenheim, and P. Deak, Appl. Phys. Lett. **117**, 032101 (2020).
17) A. Karjalainen, V. Prozheeva, K. Simula, I. Makkonen, V. Callewaert, J. B. Varley, and F. Tuomisto, Phys. Rev. B **102**, 195207 (2020).
18) J. M. Johnson et al., Phys. Rev. X **9**, 041027 (2019).
19) F. Tuomisto and I. Makkonen, Rev. Mod. Phys. **85**, 1583 (2013).
20) F. Tuomisto, A. Karjalainen, and I. Makkonen, Proc. SPIE **11687**, 1168709 (2021).
21) I. Makkonen, M. Hakala, and M. J. Puska, J. Phys. Chem. Solids **66**, 1128 (2005).
22) I. Makkonen, M. Hakala, and M. J. Puska, Phys. Rev. B **73**, 035103 (2006).
23) P. Mascher, Mater. Sci. Forum **363**, 30 (2001).
24) W.-Y. Ting, A. H. Kitai, and P. Mascher, Mater. Sci. Eng. B **91**, 541 (2002).
25) E. Korhonen, F. Tuomisto, D. Gogova, G. Wagner, M. Baldini, Z. Galazka, R. Schewski, and M. Albrecht, Appl. Phys. Lett. **106**, 242103 (2015).
26) P. Saadatkia, S. Agarwal, A. Hernandez, E. Reed, I. D. Brackenbury, C. L. Codding, M. O. Liedke, M. Butterling, A. Wagner, and F. A. Selim, Phys. Rev. Mater. **4**, 104602 (2020).
27) H. J. Wu, S. T. Ning, N. Qi, F. Ren, Z. Q. Chen, X. L. Su, and X. F. Tang, J. Appl. Phys. **130**, 195103 (2021).
28) H. J. Wu, S. T. Ning, X. B. Chen, T. Yu, T. D. Zhang, X. Qu, N. Qi, and Z. Q. Chen, ACS Appl. Energy Mater. **5**, 11441 (2022).
29) F. Tuomisto, A. Karjalainen, V. Prozheeva, I. Makkonen, G. Wagner, and M. Baldini, Proc. SPIE **10919**, 1091910 (2019).
30) V. Prozheeva, R. Hölldobler, H. von Wenckstern, M. Grundmann, and F. Tuomisto, J. Appl. Phys. **123**, 125705 (2018).
31) A. Karjalainen, I. Makkonen, J. Etula, K. Goto, H. Murakami, Y. Kumagai, and F. Tuomisto, Appl. Phys. Lett. **118**, 072104 (2021).
32) A. Karjalainen, P. M. Weiser, I. Makkonen, V. M. Reinertsen, L. Vines, and F. Tuomisto, J. Appl. Phys. **129**, 165702 (2021).
33) M. J. Tadjer et al., J. Phys. D: Appl. Phys. **53**, 504002 (2020).
34) S. K. Swain, M. H. Weber, J. Jesenovec, M. Saleh, K. G. Lynn, and J. S. McCloy, Phys. Rev. Appl. **15**, 054010 (2021).
35) J. Jesenovec, M. H. Weber, C. Pansegrau, M. D. McCluskey, K. G. Lynn, and J. S. McCloy, J. Appl. Phys. **129**, 245701 (2021).
36) B. E. Kananen, L. E. Halliburton, K. T. Stevens, G. K. Foundos, and N. C. Giles, Appl. Phys. Lett. **110**, 202104 (2017).
37) H. J. von Bardeleben, S. Q. Zhou, U. Gerstmann, D. Skachkov, W. R. L. Lambrecht, Q. D. Ho, and P. Deak, APL Mater. **7**, 022521 (2019).
38) D. Skachkov, W. R. L. Lambrecht, H. J. von Bardeleben, U. Gerstmann, Q. D. Ho, and P. Deak, J. Appl. Phys. **125**, 185701 (2019).
39) S. Bhandari, C. Nardone, and M. E. Zvanut, J. Appl. Phys. **132**, 025701 (2022).
40) Y. Qin, M. Stavola, W. B. Fowler, P. Weiser, and S. Pearton, ECS J. Solid State Sci. Technol. **8**, Q3103 (2019).
41) A. Portoff, A. Venzie, Y. Qin, M. Stavola, W. B. Fowler, and S. Pearton, ECS J. Solid State Sci. Technol. **9**, 125006 (2020).
42) A. Venzie, A. Portoff, C. Fares, M. Stavola, W. B. Fowler, F. Ren, and S. Pearton, Appl. Phys. Lett. **119**, 062109 (2021).
43) A. Venzie, A. Portoff, E. C. Perez Valenzuela, M. Stavola, W. B. Fowler, S. Pearton, and E. R. Glaser, J. Appl. Phys. **131**, 035706 (2022).

© 2023 The Author(s). Published on behalf of The Japan Society of Applied Physics by IOP Publishing Ltd